High-throughput production of silk fibroin-based electrospun fibers as biomaterial for skin tissue engineering applications

High-throughput production of Silk fibroin-based electrospun fibers as biomaterial for skin tissue engineering applications

Antonios Keirouz[1,3], Mariia Zakharova[1], Jaehoon Kwon[1], Colin Robert[1], Vasileios Koutsos[1], Anthony Callanan[2], Xianfeng Chen[2], Giuseppino Fortunato[3], Norbert Radacsi[1,*]

[1]School of Engineering, Institute for Materials and Processes, The University of Edinburgh, King's Buildings, Edinburgh, EH9 3FB, United Kingdom
[2]School of Engineering, Institute for Bioengineering, The University of Edinburgh, King's Buildings, Edinburgh, EH9 3JL, United Kingdom
[3]Empa, Swiss Federal Laboratories for Materials Science and Technology, Laboratory for Protection and Physiology, St. Gallen, CH-9014, Switzerland

*Corresponding author. Tel.: +44 (0) 131 651 7112. E-mail address: n.radacsi@ed.ac.uk

ABSTRACT

In this work, a nozzle-free electrospinning device was developed to obtain high-throughput production of silk fibroin-based trinary biocompatible composite fibers with tunable wettability. Synthetic fiber materials tend to present suboptimal cell growth and proliferation, with many studies linking this phenomenon to the hydrophobicity of such surfaces. In this study, electrospun mats consisting of Poly(caprolactone) blended with variant forms of Poly(glycerol sebacate) and regenerated silk fibroin were fabricated. The main aim of this work was the development of fiber mats with tunable hydrophobicity/hydrophilicity properties depending on the variant curing forms and concentration of PGS. A variation of the conventional protocol used for the extraction of silk fibroin from *Bombyx mori* cocoons was employed, achieving significantly increased yields of the protein, in a third of the time required via the conventional protocol. The wettability of the scaffolds could be modulated varying the ratios and curing time of the PGS within the composite fibers. The trinary composite biomaterial presented good *in vitro* fibroblast attachment behavior and optimal growth, indicating the potential of such constructs towards the development of an artificial skin-like platform that can aid skin regeneration.

KEYWORDS: Poly(glycerol sebacate); Poly(caprolactone); silk fibroin; nozzle-free electrospinning; fibroblasts

1. INTRODUCTION

Tissue-engineered skin substitutes and advanced wound dressing biomaterial require several criteria to be met. First, they need to be biocompatible to overcome immune rejection and inflammation.[1] Second, an appropriately hydrophilic interface between the tissue and the biomaterial is required, which effectively facilitates cell adhesion and proliferation. Third, the construct needs to be lightweight to

minimize foreign body sensation, biodegradable, and facilitate an architecture that allows for the appropriate water retention, nutrient transport, breathability, and structural stability that offers an optimal regenerative niche.[2,3] To satisfy these requirements, a range of biocompatible materials have been extensively studied, focusing on wound management and skin tissue repair.[4] Among them, electrospun materials are favorable towards the reconstruction of porous skin tissue-like scaffolds as they allow the development of structures that closely resemble the native extracellular matrix (ECM), where cells can adhere, proliferate, freely migrate, and induce neovascularization.[5,6] Electrospinning is a well-established technique that can be ideal for the fabrication of such a construct in the form of non-woven networks of fibers.[7] The electrospun fiber morphology, granted by the micro- and nano-dimensions, can facilitate the absorption of exudate and efficient gas exchange while being capable of modulating the orientation of the cells and promoting cellular attachment and proliferation.[8,9] These features can ultimately provide and improve the care, recovery, and healing requirements of the injured skin tissue.

A major problem faced in the development of such constructs today surrounds the meager production rates of this process and the principal use of synthetic hydrophobic polymeric material. One can apprehend that a polymer system integrating the unique properties of different materials can provide distinct features to the final composite structure. Considering this, a unique composite structure, based on electrospun fibers, consisting of synthetic and naturally-derived material, was developed. Nonetheless, finding the appropriate solvent system, obtaining the desired critical entanglement concentration of each polymer and the required viscosity (below the overlap concentration of the polymer-system) to achieve a stable and consistent jet during electrospinning can be challenging.

Bombyx mori silkworms have been domestically bred and part of the textile industry for centuries.[10] Silk fibers are protein-based fibrous biopolymers, formed of repetitive hydrophobic motifs of hexapeptides that consist of $[Gly\text{-}Ser\text{-}Gly\text{-}Ala\text{-}Gly\text{-}Ala]_x$, which form a stable anti-parallel beta-sheet structure with [Gly–Ala/Ser] dipeptides.[11,12] The strong hydrogen bonding between the beta-sheets of silk fibroin (SF) contributes to the semi-crystalline structure of the macromolecule; these properties make SF mechanically superior to most bio-derived polymers.[13,14] It has been shown that SF is a valuable material for the development of wound healing dressings because it has excellent biocompatibility, good oxygen and vapor permeability while inducing minimum inflammatory responses.[15,16]

Poly(glycerol sebacate) (PGS) is a biocompatible and biodegradable thermoset elastomer that has emerged as a promising material for soft tissue engineering. Nonetheless, electrospinning neat PGS into homogenous fibers is an arduous process because its low molecular weight does not allow chain entanglement of the pre-polymer and the high viscosity of the cured polymer makes it insoluble in most organic solvents.[17] On the other hand, Poly(caprolactone) (PCL) is a well-established polymer in electrospinning as it can steadily produce fibers. However, PCL is hydrophobic, and pure PCL fibers lead to suboptimal cell adhesion and proliferation.[18,19]

To make use of the advantages of each material, in this study, we systematically studied and employed the nozzle-free electrospinning technique to blend these components, tune andcharacterize their properties to demonstrate the effectiveness of composite electrospun structures towards tissue engineering. In our work, non-acrylate PGS was blended with a *B. mori* fibroin-acidic system, and PCL was incorporated as a backbone-polymer carrier to stabilize and improve the spinnability of the composite solution. This study focuses on the development of PCL-backbone SF-PGS composite blends that could be used for the development of artificial skin constructs with adjustable wettability properties and improved viability. A high-throughput nozzle-free electrospinning apparatus was used, and the production rate was compared against a commercial needle electrospinning device. For the extraction of SF from *B. mori* cocoons, a variation of the traditional approach was developed that was found to yield much larger quantities than the conventional molecular cassette cutoff method at a third of the time needed.[20] The morphological properties and chemistry of the developed mats were assessed. A degradation study was conducted, and contact angle measurements examined the effects that PGS and SF have at increasing the hydrophilicity of the composite PCL fibrous scaffolds. Immortalized (telomerase reverse transcriptase) human dermal fibroblasts (HDF) were used to examine the seeding efficiency, adhesion properties and proliferation of this dermal cell-line.

2. MATERIALS AND METHODS

2.1 Materials and cells

Bombyx mori silkworm cocoons were obtained from local sericulture (Oliver Twists Threads Ltd., Kirk Merrington, UK). Sebacic acid (≥98%, M_w = 202.20 g/mol), and glycerol (≥99%, M_w = 92.09 g/mol) were purchased from Alfa-Aeser, UK. Poly(caprolactone) PCL $(C_6H_{10}O_2)_n$ (M_w = 80,000 g/mol) was purchased from Sigma-Aldrich, UK. 1,1,1,3,3,3-Hexafluoro-2-propanol (HFIP) was obtained from Fluorochem, UK. Solvents: absolute ethanol (≥99.5%, EtOH), chloroform (≥99.8%, CF), and formic acid (99%) were purchased from Acros Organics, UK, whereas salts: calcium chloride ($CaCl_2$), sodium carbonate anhydrous (Na_2CO_3), and lithium bromide (LiBr) were purchased from Thermo-Fisher Scientific, UK.

Immortalized human skin fibroblasts (hTERT, MRC Centre for Cardiovascular Science, Edinburgh, UK) was used for the cell culture experiments. High glucose, pyruvate, Dulbecco's Modified Eagle Medium (DMEM), fetal bovine serum albumin (FBS), non-essential amino acids, penicillin-streptomycin, and Hanks' Balanced Salt Solution (HBSS) were purchased from Thermo-Fisher Scientific, UK. Glutaraldehyde, hexamethyldisilazane (HDMS), and sucrose were purchased from Alfa-Aesar, UK.

2.2 Extraction of silk fibroin

SF was extracted from *B. mori* silkworm cocoons by a newly developed alcohol precipitation method.[21] Sericin was removed by degumming 10 g of cocoons in 0.02 M Na_2CO_3 solution at 100 °C

for 30 min. The degummed silk cloth was then rinsed thoroughly in deionized water and left to dry under the hood overnight. The woven silk filaments were then dissolved in 9.3 M LiBr aqueous solution for 4 h at 50 °C in a narrow beaker to regenerate the SF.

Instead of continuing with the conventional protocol, where the chaotropic LiBr salt is removed by dialysis using molecular weight cutoff cassettes[21], ethanol precipitation was used to separate LiBr from the SF. To achieve an efficient degree of fibroin precipitation, the volume of ethanol was thirty times that of the aqueous SF-LiBr solution. After stirring the dropwise dispersed SF solution in ethanol for 1 h, the SF residues were attained by filtration (Whatman grade 1573) and washed with ultrapure water. The filtered SF was considered LiBr-free when the electrical conductivity of the filtered water was equal to the electrical conductivity of the ultrapure water prior to washing (≤ 0.1 µS/cm). This was further confirmed by XPS of the produced electrospun mats. The paste-like wet silk fibroin was dried at 50 °C and milled to form a powder (**Figure 1**).

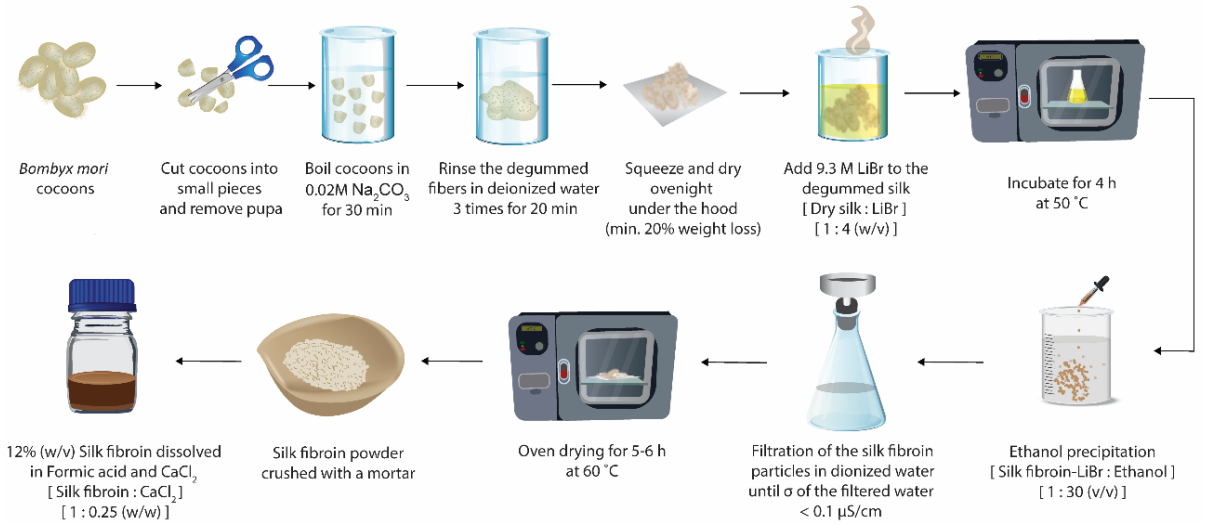

Figure 1. Silk fibroin extraction and processing to regenerated form. Initially, *B. mori* cocoons are cut into small pieces and degummed in 0.01 M solution of Na_2CO_3 at 100 °C for 30 min. The degummed silk is rinsed in deionized water 3 times for 20 min each, and it is left to dry at room temperature overnight. Then, 9.3 M LiBr solution is added to the dried silk fiber mesh at a ratio of 1:4 SF:LiBr solution (w/v) to dissolve the fibroin. The LiBr-SF solution is placed into the oven for 4 h at 50 °C. Afterward, the SF is precipitated by gradually dripping the SF-LiBr solution in pure ethanol until it reaches a ratio of 1:30 SF-LiBr:EtOH (v/v), and it remains under agitation for 1 h. Subsequently, SF residues are removed by filtration and washed with ultrapure water. The purified SF is oven-dried at 50 °C. Dried SF is milled into powder with a mortar and dissolved in Formic acid /$CaCl_2$ to obtain the final SF concentration of 12% (w/v).

2.3 Polymer solution preparation and nozzle-free electrospinning

PGS was synthesized based on the initially published polycondensation method.[22] The pre-polymer PGS (pPGS) was produced by thoroughly mixing equimolar (1:1 M) glycerol and sebacic acid at 120 °C under N_2 gas purged at a flowrate of approximately 120 $cm^3.min^{-1}$, using a round bottom three-necked reactor at reduced pressure (1 Torr) for 24 h. The partially cross-linked form of the polyester,

PGS, was then obtained by steadily reducing the pressure to 40 mTorr, at the same temperature for an additional 48 h, under a reduced atmosphere. No exogenous catalysts were used for this process. PGS and pPGS 15% (w/v) were dissolved separately in HFIP while still in the viscous liquid phase of the polymer by pouring it directly from the three-neck flask prior to cooling off.

PCL 15% (w/v) was dissolved in a solvent system consisting of 80:20 (w/w) HFIP: Formic acid. To prepare the SF solution 12% (w/v), silk fibroin powder was dissolved in a solution of $CaCl_2$ and Formic acid. The ratio of SF: $CaCl_2$ was 1:0.25 (w/w).[23] All solutions were magnetically stirred (350 rpm) overnight at room temperature.

After homogenous solutions were obtained, trinary blend compositions of PCL-backbone SF:PGS, and PSF:pPGS solutions were prepared. The mass ratio of SF was kept constant for all the blends. Binary blends of SF:PGS and SF:pPGS were also prepared. The blends containing a solvent system consisting of HFIP: Formic acid: $CaCl_2$ were magnetically stirred overnight at room temperature before electrospinning, and the electrical conductivity and pH of the polymer solutions were measured before every experiment. Table 1 indicates the mass ratios for each trinary and binary blend.

Table 1. Blend compositions. Trinary PCL-backbone SF:(p)PGS, binary blend SF:(p)PGS and PCL solutions. Final concentration of 13.5% (w/v) for the trinary blend, 21% (w/v) for binary blends, and 7.5% for the PCL.

Polymer blend	**Ratio [w/w]**		
	Silk fibroin 12% (w/v)	**PCL 15% (w/v)**	**PGS 15% (w/v)**
SF:PCL:PGS	1	0.75	0.25
&	1	0.50	0.50
SF:PCL:pPGS	1	0.25	0.75
SF:PGS	2	-	1
SF:pPGS	2	-	1
PCL	-	1	-

Fibers were produced using an in-house built nozzle-free electrospinning device, comprised of a rotating cylinder electrode submerged within a Teflon pool, where the polymer solution was placed, and a biased rotating collector electrode under constant N_2 flow. A high-voltage power supply with a potential difference of 60 kV (+30/-30 kV) was applied between the two rotating electrodes, which spurred the formation of multiple Taylor cones along the rotating electrode surface, resulting for jets to stretch forming fibers in an upward motion.[24] The process is illustrated in Figure 2. Electrospinning experiments with PCL were also carried out using a commercial electrospinning device (IME, Netherlands), in order to compare the production rate by measuring the dry fiber weight of electrospun mats.

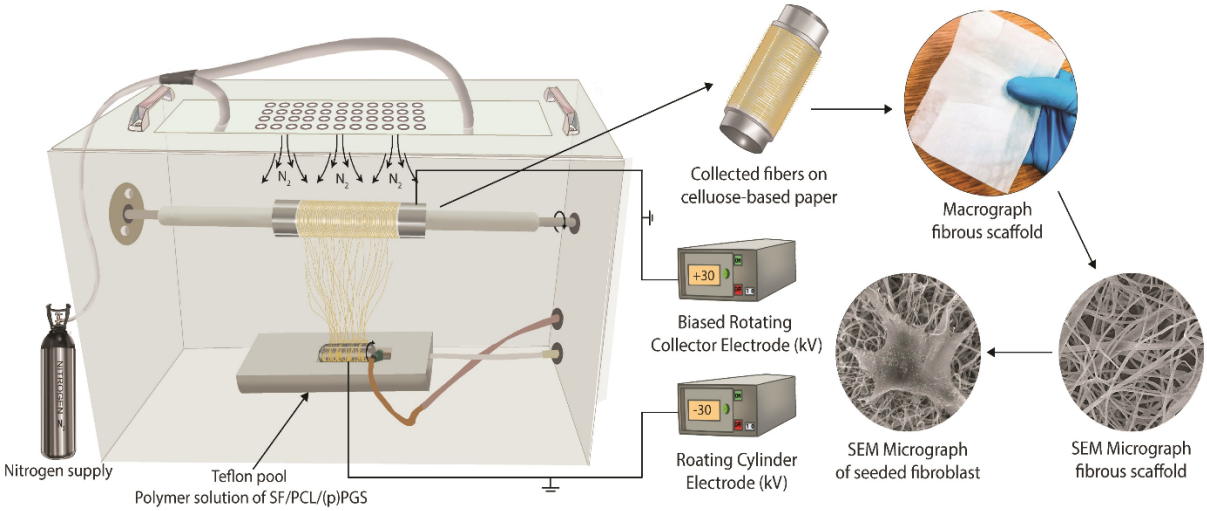

Figure 2. Schematic representation of the nozzle-free electrospinning process, showing a macrograph of the produced fibrous scaffold and the SEM micrographs of the fibers with and without fibroblasts.

2.4 Degradation and wettability

For each electrospun mat, five specimens were cut into 5 × 5 mm^2 pieces obtained from three independently electrospun mats, adapted to a previously published protocol.[25] Subsequently, the scaffolds were immersed in ethanol for 2 h to increase the net amount of β-sheet blocks. The samples were then weighed (initial mass, W_o) and placed in Petri dishes containing PBS (1×, pH 7) at room temperature under ambient conditions, and the solution was refreshed daily. After being immersed for predetermined times, the specimens were dried at 50 °C and weighed (dry mass post submersion, W_i). The residual mass (weight loss, μ) of each specimen was calculated based on Equation 1:

$$Weight\ loss\ (\mu)(\%) = \frac{(Wo-Wi)}{Wo} \times 100 \qquad \textbf{(1)}$$

The wettability properties of the different composite membranes were determined by static water contact angle measurements at room temperature. The surface was characterized by the sessile drop technique, using a drop shape analyzer (DSA100, Kruss, Germany). Briefly, 5 μL deionized water droplets were settled in the center of an orderly unswerving fiber mat. The data were analyzed on Advance by Kruss and ImageJ.

2.5 Morphological and chemical characterization

The fiber structure, surface morphology, and porosity of the electrospun mats were evaluated by scanning electron microscopy (JSM-IT100, JEOL, Japan). For the cell-containing scaffolds, the specimens were first rinsed in warm Hank's balanced salt solution and then fixed overnight at 4 °C with 3% (v/v) glutaraldehyde that was prepared in an SEM buffer consisting of Na-phosphate and 0.1 M sucrose at pH 7.4. The scaffolds were thoroughly washed in the SEM buffer, and gradually dehydrated in EtOH (20%, 35%, 50%, 70%, 95% and 100%, v/v) for 15 min increments, and then left to dry in

Hank's balanced salt solution overnight chemically. The dried specimens were sputtered with 10 nm Au. The fiber diameter and pore size were calculated from random measurements (n > 100) using ImageJ.

The ultrastructure of the seeded scaffolds and the in-depth cellular expansion were observed by Zeiss Crossbeam 550 focused ion beam (FIB) incisions *via* scanning electron cryomicroscopy (cryo-SEM, Carl Zeiss, Germany). FIB images were obtained at 30 kV, 300 pA, at an accelerating voltage of 3 kV.

Fourier-transform infrared with attenuated total reflectance (ATR-FTIR) spectrophotometry was used to determine the chemical composition of the electrospun mats (Varian 640-IR, Varian Medical Systems, USA). For each vacuum dried specimen, 72 scans with a 2 cm^{-1} resolution and a spectral range of 4200-600 cm^{-1} were collected. Silk fibroin region-specific scans ranging from 2000-600 cm^{-1} were also obtained.

The surface chemistry of the electrospun scaffolds was analyzed with X-ray photoelectron spectroscopy (XPS) taken by a PHI 5000 VersaProbe II (USA), using an Al Kα X-ray source. The energy resolution of the spectrometer was set to 0.8 eV/step at a pass-energy of 187.85 eV for the survey scans. Carbon at 284.5 eV was used as a reference to correct charge effects. The elemental compositions were determined using instrument dependent atom sensitivity factors. The photoelectron-transitions of C1s, O1s, N1s, Ca2p, Cl2p, and Si2p were selected to determine the elemental concentrations. Data analysis was performed using the CasaXP software (Casa Software Ltd, United Kingdom).

2.6 *In vitro* fibroblast proliferation

The immortalized human skin fibroblasts (HDF-TERT) were cultured in high glucose-pyruvate DMEM medium supplemented with 10% FBS, 1% Penicillin-Streptomycin, and 1% L-Glutamine; the culture was maintained in a humidified atmosphere (37 °C and 5% CO_2), with the medium being replaced every two days.

The electrospun mats were punched in 8 mm circular pieces and treated with ethanol for 2 h to promote crystallization of the fibroin protein. The scaffolds were then sterilized in 70% (v/v) ethanol for 24 h, washed thoroughly with PBS, and pre-soaked in DMEM for 48 h. The cells were seeded in a 20 µL medium suspension containing 2×10^5 fibroblasts/scaffold in 24-well tissue culture plates. The seeded scaffolds were left still for 2 h under the hood and then 4 h within the incubator before adding the supplementary media, in order to promote cellular adhesion. The media were discarded and replaced every second day in a manner of 50/50 fresh/old.

The quantitative proliferation of cellular attachments was examined 1, 3, 5, and 7 days after seeding using the Alamar blue cell viability assay according to the manufacturer's instructions. At least 3 scaffolds with adherent cells were examined for every trinary scaffold. Cells cultured directly on tissue-treated plates acted as the control. The seeded scaffolds were washed with PBS, and 10% (v/v) Alamar Blue reagent in DMEM was added for 4 h at 37 °C and 5% CO2. The reduced Alamar blue suspension of 100 µL was pipetted and transferred in triplicates onto a 96-well dark plate and read with an ELISA

spectrophotometer. The percentage of Alamar blue reduction was calculated for each group, as well as the fold reduction in comparison to the first day of culture.

All quantitative data are shown as mean ± standard deviation (SD). Statistical significance between the different groups was analyzed by repeated measures or one-way analysis of variance (ANOVA), with confidence interval adjustment Bonferroni, using SPSS v.24 (IBM, USA).

3. RESULTS AND DISCUSSION

3.1 Electrospun scaffold morphology

The fibrous constructs were electrospun using the nozzle-free electrospinning apparatus described above, where the fibers were collected on cellulose (baking) paper. Table S1 summarizes the electrospinning and solution parameters.

When incorporating SF with other synthetic polymers, it is important to consider the inter/-intramolecular interactions that lead to the formation of the fibroin β-sheets.[26] The temperature, pH, fibroin and salt concentration, shear viscosity, and the solvent system used were optimized to prevent gelation of the binary and trinary spinning solutions upon blending.[27,28]

The morphological properties of the trinary SF:PCL:(p)PGS and binary SF:(p)PGS blends of different ratios were determined by SEM imaging (Figure 3). The distribution curves of the binary and trinary electrospun fibers, along with the fiber diameter and pore size values can be found in Figure S1 and Table S2. The concentration of the PGS within the blends played an important role in the morphology of the produced fibers. The images show a clear difference in the fiber diameter values between the scaffolds prepared with the two variant forms of PGS synthesized. It was apparent that the trinary SF:PCL scaffolds containing PGS tend to have a higher average fiber diameter ranging from 4.1 ± 3.0 μm 2.11 ± 1.34 (Figure 3C-E), while the pPGS scaffolds presented values in the range of 1.62 ± 0.80 μm to 1.42 ± 0.66 μm (Figure 3F-H). Moreover, the average fiber diameter was noticeably increased in blends with a higher ratio of PGS (e.g., the ratio 1:0.25:0.75 resulted in the thickest 4.1 ± 3 μm fibers; Figure 3C).

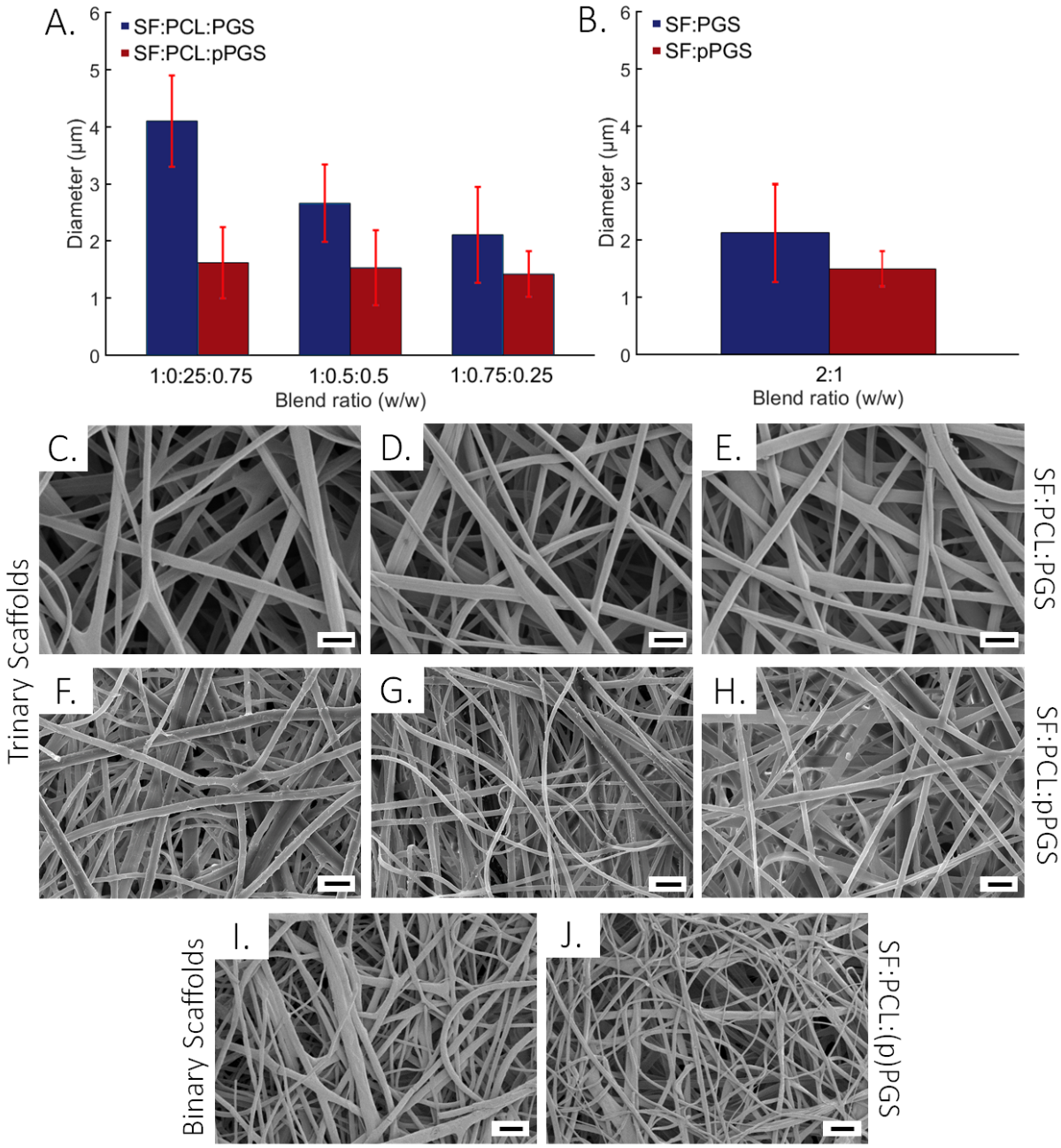

Figure 3. Average diameter values of the **(A)** trinary SF:PCL:PGS and SF:PCL:pPGS and **(B)** binary SF:PGS and SF:pPGS blends. Representative SEM micrographs of the trinary SF:PCL:PGS **(C-E)**, SF:PCL:(p)PGS **(F-H)**, and binary SF:PGS 2:1 (w/w) **(I)**, SF:(p)PGS 2:1 (w/w) **(J)** scaffolds. The images were obtained after drying the ethanol-treated electrospun mats at 32 °C. Scale bar 10 µm.

The PGS is initially difficult to electrospin due to its low viscosity. Moreover, pPGS glass transition is below room temperature; therefore, the fiber can be easily fused during the electrospinning process, thickening the produced fibers. The pPGS form of the elastomer was found to produce fibers with a mean fiber diameter that decreased by 23-65%, depending on the corresponding blend ratio. These results indicate the effect of the elastomeric PGS on the fiber morphology.

The mean pore size (Table S2) of the trinary blends containing PGS was on an average twice that of the pPGS-containing electrospun mats, with no significant difference existing for the varying concentration of PGS within the blends. The SF:PCL:PGS presented a mean pore size of 15.6 ± 7.1 μm (porosity 74 ± 5.4%), while the SF:PCL:pPGS 9.1 ± 5.7 μm (porosity 61 ± 7.4%). Along with the choice of biomaterial, the pore size needs to be considered for the development of a scaffold capable of promoting cell migration, adhesion and promote cell-to-cell contact. [29,30] The optimal pore size for fibroblast ingrowth is 5-15 μm with wider interconnected pores, further facilitating the diffusion and ingrowth of nutrients on the site.[31] Thus, the trinary blends fall within the optimal pore size for good cellular infiltration. While the porosity of the produced mats falls within the required gradient for tissue reorganization and governing an effective tissue regeneration, it can also negatively affect the mechanical stability of the construct. Consequently, the addition of PCL within the trinary blends is widely considered as a good approach to stabilizing fiber-based biomaterial.[32,33]

To further analyze the effect of PGS on SF itself, binary blends of SF:(p)PGS and SF:PGS with the ratio 2:1 (w/w) were electrospun using the same apparatus under the same conditions. In contrast to the PCL containing fibers, the distribution of the fibers produced by the binary blends were found to be more spread out, losing their uniformity. The fiber diameter of SF:PGS was 2.13 ± 1.50 μm (Figure 3I), while the fiber diameter of SF:(p)PGS was 1.04 ± 0.30 μm (Figure 3J). The SF:(p)PGS fibers appear to carry a finer fiber morphology compared to the PGS counterparts, but some fusion of fibers was still apparent. According to several studies, crosslinking pPGS increases the molecular weight, which results in restriction of chain mobility, increased entanglement, and higher internal fluid friction that makes jet extension harder.[34] This leads to the binary and trinary blends, containing PGS to form thicker fibers. Furthermore, the correlation of viscosity with fiber diameter was confirmed in the studies of Drew et al.[35] and Fong et al.[36], where increasing the solution viscosity tends to increase fiber diameter during electrospinning.

When comparing the blends with or without incorporating PCL, both PCL-containing groups present smooth fibers, but with an increased fiber diameter compared to the SF:PGS and SF:(p)PGS blends in most cases; this could be attributed to changes in the dielectric constant of the blend when PCL is added. Generally, the dielectric constant of a solvent also plays a significant role in the electrospinning process: the higher the dielectric value, the lower the diameter of the resultant electrospun fibers.[37] PCL was dissolved in a binary solvent system containing HFIP: Formic acid 80:20 (w/w), as formic acid has a higher dielectric constant than HFIP, the mix of these two solvents may increase the electrical conductivity of the PCL blend solution, contributing to the fabrication of smoother fibers during electrospinning.[38]

The nozzle-free setup with a cylinder spinneret had higher fiber productivity and required fewer operational costs compared to a conventional single or multi-needle spinneret.[39,40] However, it is comparatively more complex, as there is a range of new electrospinning parameters to be considered, including, but not limited to, the spinneret rotating speed, electric field distribution, and spinneret

geometry. Niu et al.'s study[40] found that the electric field intensity reaches the highest values at the ends of the cylinder spinneret and decreases towards the center, which may hamper jet formation.

3.2 Production rate of the nozzle-free device

Nozzle-free electrospinning allows jets to form and stretch from multiple locations at once, thus significantly increasing the production rate compared with conventional needle-based devices. While electrospun fibers are vastly suitable for the fabrication of tissue engineering constructs, the low yield of the needle-based electrospinning devices limits the ability to scale up the production, even if this may not constitute a problem in a laboratory setting. The development of multi-needle apparatuses was proven ineffective due to overlapping electrostatic forces between the needles, affecting the travel path of the independent Taylor cone jets.[41] The production rate of the in-house built nozzle-free apparatus developed for this study was compared with a commercial single nozzle electrospinning device under optimal conditions for an hour using 7.5% (w/v) PCL. As illustrated in Figure 4, the nozzle-free device produced fibers at an increased rate that corresponds to an 11-fold factor of dry fibers compared to the conventional device. These findings are in agreement with previously published work.[42]

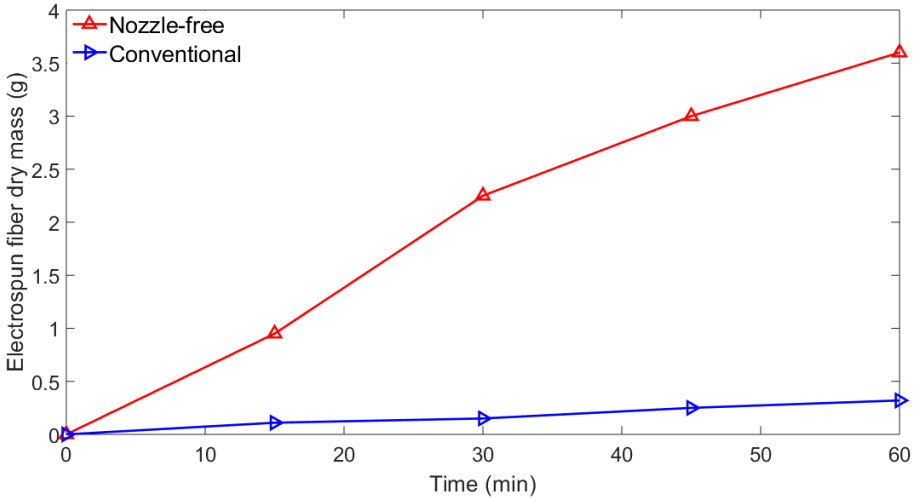

Figure 4. Comparison of the production rate between the in-house built nozzle-free electrospinning device, and a commercial needle-based electrospinning device. PCL 7.5% (w/v) in HFIP. Nozzle-free electrospinning: 60 kV, conventional electrospinning: 16 kV (+12/-4, 10 µL/min), needle tip-to-collector distance 15 cm.

3.3 Influence of PGS in the degradation properties of the electrospun mats

The PGS specimens (Figure 5A, Table S3) retained most of their original mass within 3 days of incubation with a minimum weight loss of 3% at 30 min incubation and a maximum weight loss of 42.6% after a month. Within this group, there is a clear trend of mass loss when decreasing the amount of PCL within the scaffolds.

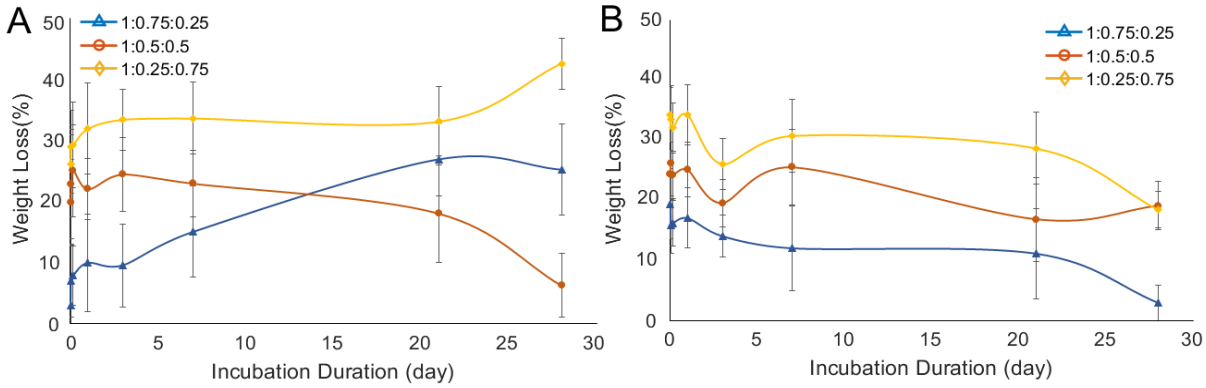

Figure 5. Percentage of mass loss of the PGS group at varying incubation periods. Blend (w/w) ratios of **(A)** SF:PCL:PGS, and **(B)** SF:PCL:(p)PGS.

A similar pattern is seen in the pPGS group (Figure 5B, Table S3), where the samples with the lower PCL ratios presented higher degrees of degradation. This is supported by Liu et al.'s findings of the PCL's slower degradation rate compared to PGS [43]. Therefore, by using the two variant forms of PGS, and by adjusting its ratio within the polymer blends, it can help control, to a certain extent, the degradation of the composite electrospun mats. This can eventually assist the breakdown of the ECM-like fiber structure at an appropriate rate that can complement the natural ECM reorganization during the wound healing process.

The initial lack of degradation of the PCL-backbone SF:PGS blends was expected since many studies have shown that PCL resists degradation by hydrolysis due to its hydrophobic nature. [44–46] Polyesters such as PCL degrade significantly faster via enzyme-mediated hydrolysis [44] and have been shown to have poor degradation behavior in PBS.[45] The degradation results align with Nadim et al.'s findings where only 26% mass loss was recorded over 30 days on a fibrous PCL:PGS mat of equal mass ratio [47], which is similar to the degradation behavior seen for the 1:0.5:0.5 group in this study (Figure 5). The reported weight loss of the SF:PCL:PGS scaffold may be lower in contrast to Nadim et al.'s results due to the incorporation of SF into the blend, making it more resistant to degradation, thus illustrating the effect of integrating a natural polymer within the composite.[48]

One of the advantages of utilizing SF stems from its stability in the presence of water, which may prevent the premature dissolution of blends. Furthermore, ethanol treatment of the acid-based SF blends promotes the formation of hydrogen-bonding β-sheet structures (silk II), which can manipulate the hydrophilicity and improve the scaffold's degradation in aqueous environments. [48,49] A macroscopic assessment of the trinary electrospun mats post Ethanol treatment, can be observed in Figure S2. Silk II structures have been shown to exhibit higher hydrophobicity via contact angle measurements conducted by Jin et al.[49], which has indicated greater stability in PBS solution. This would explain the lower degradability of the trinary SF:PCL:PGS composite fibers, incorporating SF, to that of the binary PCL:PGS fibrous mats.

Initially, it was believed that with more extended incubation periods, the scaffolds would have had more time to hydrolyze, thus presenting an increased mass loss. While this is seen to be the case for the

PGS groups, the opposite appears to occur with the pPGS groups, where an inverse correlation between incubation time and degradation can be observed. A clarification needs to be taken into account when considering that the data displayed in Figure 5 refer to the average values of the actual degradation of each specimen measured rather than the sum, where previous points are added after each measurement.

A higher degree of esterification density within the PGS structure was expected to hamper degradation compared to the pPGS, but no significant difference was observed in the mass loss between the PGS and pPGS blends regarding the minimum and maximum weight loss, which aligns with the findings of Pomerantseva et al.'s.[50] However, they reported that water uptake decreased when the curing time of PGS increased; hence it can be suggested that pPGS has a lower degradability compared to PGS. Further, it was mentioned that the water uptake of PGS decreases as the curing time of the elastomer increases.[50] Hence, the pPGS group has a greater capacity to take up water, and it may have retained its mass of water even after the dehydration process, explaining the lower mass loss of pPGS compared to PGS. The scaffold's ability to retain water can be associated with its wettability, which is known to be one of the few main factors governing protein adsorption and cell adhesion [51–53].

A dressing that readily takes up water may dehydrate the wound bed making it more prone to scarring, whereas the low degree of retention may increase the risk of infection and halt the healing process due to the build-up of exudates in the wound bed, thus finding the balance between the two is challenging. [53]

These results have shown that the incorporation of silk fibroin, PCL, and PGS in a composite fibrous mat can be used to influence the upper and lower bounds required towards finding appropriate conditions for controlling the rate of degradation on the site.

3.4 Wettability

Surface wettability is a crucial characteristic of polymeric biomaterials, which plays critical roles in cellular adhesion, proliferation, migration, and survival [54]. These interactions between the biomaterial and cells can be especially important when determining whether a construct or a device can regulate inflammatory responses and the degree of tissue adhesiveness.[55] Cell attachment is mostly governed by alterations in surface energy - higher energy hydrophilic surfaces encourage adhesion, whereas low surface energy substrates typically inhibit cellular adhesion.[52] It has been shown that moderately hydrophilic/hydrophobic surfaces are favorable towards the adsorption of surface proteins that mediate cellular adhesion and offer downstream signaling to specific cell adhesion receptors, which are in turn induce the deposition of ECM structural components required for tissue formation and regeneration.[52,56] Moderately hydrophilizing a hydrophobic surface, such as PCL, can alter the surface energy of the biomaterial improving the adsorption of surface-related proteins and the diffusion of nutrients, which can lead to optimal adhesion, increased cellular infiltration, and tissue in-growth in a wounded area. [57]

The contact angles (CA) were determined for each binary, trinary, and PCL scaffold to investigate the effect that PGS and SF can have on the hydrophobicity of PCL (Figure 6). Figure S2 presents the

contact angle values for each group examined upon a 5 μL droplet settling at the surface of the electrospun mats over time, and significant differences among the groups examined. The hydrophobicity of the PCL-only fibers was confirmed with a high contact angle of 125.9° ± 6.5°. The hydrophilicity/hydrophobicity ratio of a fibrous scaffold affects the adhesion and proliferation behavior of the cells.[58] By integrating natural polymers along with synthetic hydrophobic polymers, such as PCL – it is possible to reduce the contact angle of the fibers and improve the hydrophilicity of the final construct. Silk fibroin fibers can be very hydrophilic due to the high number of amino acid and carboxylic domains they contain.[59]

The random coil conformation of the fibers can be stabilized by adding Ca^{+2}, which causes the formation of β-sheets with Ca^{+2} between the fibroin domains during both the electrospinning process and post-treatment with ethanol (Figure S2). [60,61] Furthermore, PGS is well known for its hydrophilicity due to the hydroxyl groups present on the polyester's backbone. The titration of the total acid number can be varied by functionalizing the elastomer, making it possible to increase the hydrophilicity.[62,63] As the number of ester linkages increases during the curing process, it is expected that PGS will add increased hydrophilicity to the composite scaffolds, compared to its pre-polymerized counterpart.

As Figure 6 indicates, the addition of higher concentrations of PGS in the composite electrospun membranes increased the wettability of the corresponding scaffolds accounting a period of 30 s. Additionally, it is apparent that higher concentrations of PGS made the trinary scaffolds more rapidly absorbable in comparison to the corresponding pPGS mats. In the binary SF:PGS and SF:pPGS scaffolds with a CA of 83° ± 1.56° and 124.5° ± 8.02°, respectively, it is once again shown that the PGS form of the elastomer induces further wettability and a lower CA than the pre-polymerized form. **Figure S3** shows the contact angle measurements for each group 0 and 5 seconds after applying the deionized water droplet.

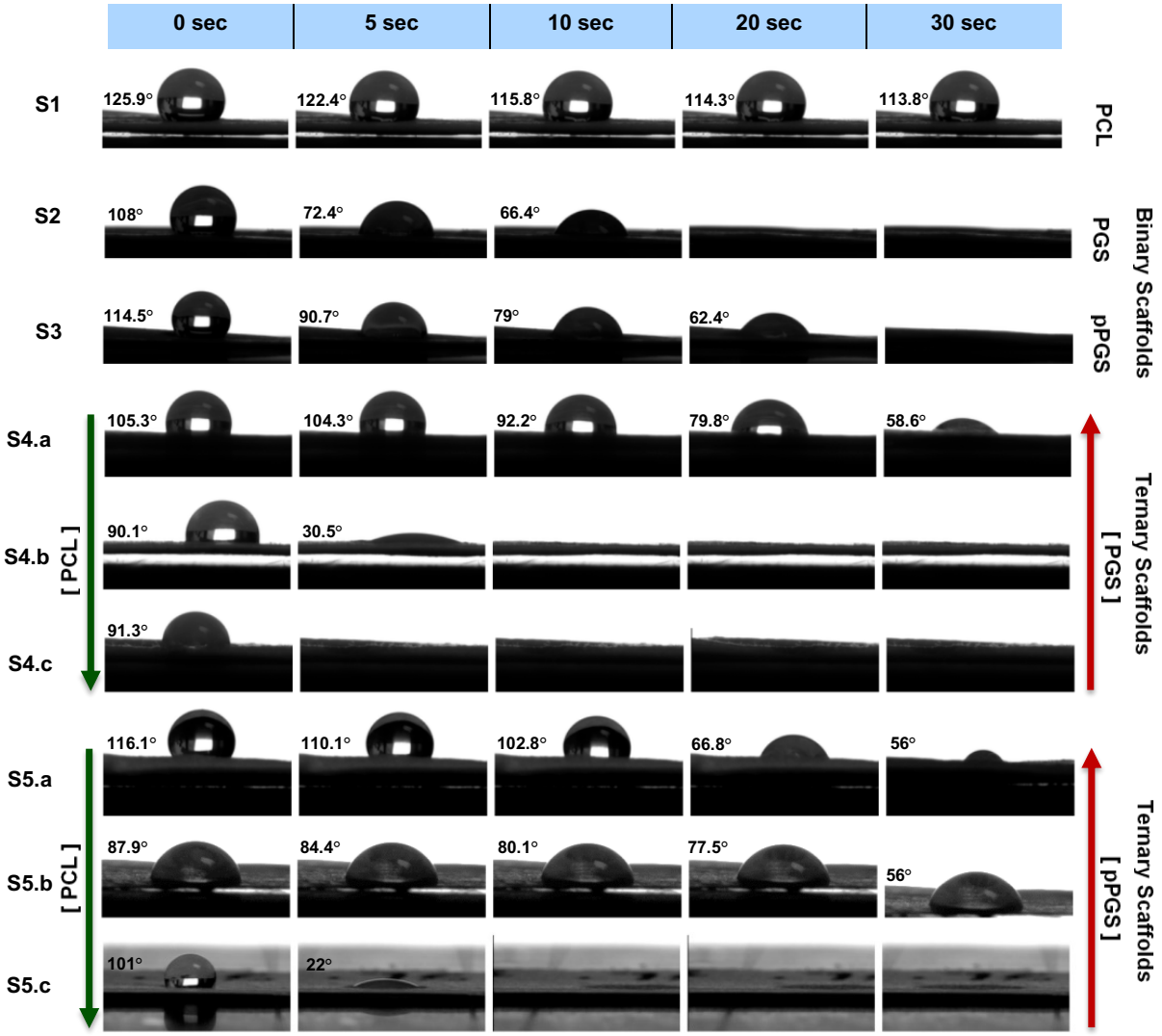

Figure 6. Water contact angle over time. PCL, binary SF:PGS, SF:pPGS and trinary PCL-backbone SF:PGS and SF:pPGS electrospun mats. Time intervals 0, 5, 10, 20 and 30 s. S1: PCL, S2: SF:PGS, S3: SF:pPGS, S4: PCL-backbone SF:PGS, S5: PCL-backbone SF:pPGS. Letters indicate the ratio of the trinary blends, where the SF:PCL:(p)PGS ratio is (a) 1:0.75:0.25, (b) 1:0.50:0.50, (c) 1:0.25:0.75. Red arrows (p)PGS and green arrows PCL. Brackets indicate concentrations.

3.5 Cell adhesion, viability, and proliferation

Human dermal fibroblasts were passaged in supplemented Eagle's minimal essential medium and seeded on the electrospun mats. Figure 7A depicts the cell growth and expansion in the electrospun SF:PCL:(p)PGS mats for each blend 1, 3, 5, and 7 days after the initial seeding. Alamar blue cell viability assay was used to assess the viability and number of cells. Viable cells reduce the non-fluorescent Resazurin (blue) to a fluorescent red-colored complex called resorufin. The cells' metabolic activity is equivalent to the viability of the cells, where they act as an electron acceptor for enzymes (NADP and FADH) during oxygen consumption.[64] As growth follows the same pattern with no significant difference at the extent with which the seeded cells reduced the reagent between the pPGS and PGS, the results were merged for clarity.

The proliferative properties of the SF:PCL:(p)PGS electrospun membranes were analyzed by establishing the relation between the growth of cells and the period of incubation. The cell viability of the cells on the electrospun mats having concentrations of SF:PCL:(p)PGS in the ratio of 1:0.5:0.5, 1:0.25:0.75, and 1:0.75:0.25 were studied and compared with PCL-only electrospun mats. The fibers appear to gradually expand on the trinary scaffolds with a significant ($p<0.05$) increase in the number of cells as the number of days in culture increased when compared with the PCL-only group. This linear increase in the cell viability was apparent for all the blends that were examined. Thus, the composite fibers appeared to provide a matrix where fibroblasts can proliferate rapidly.

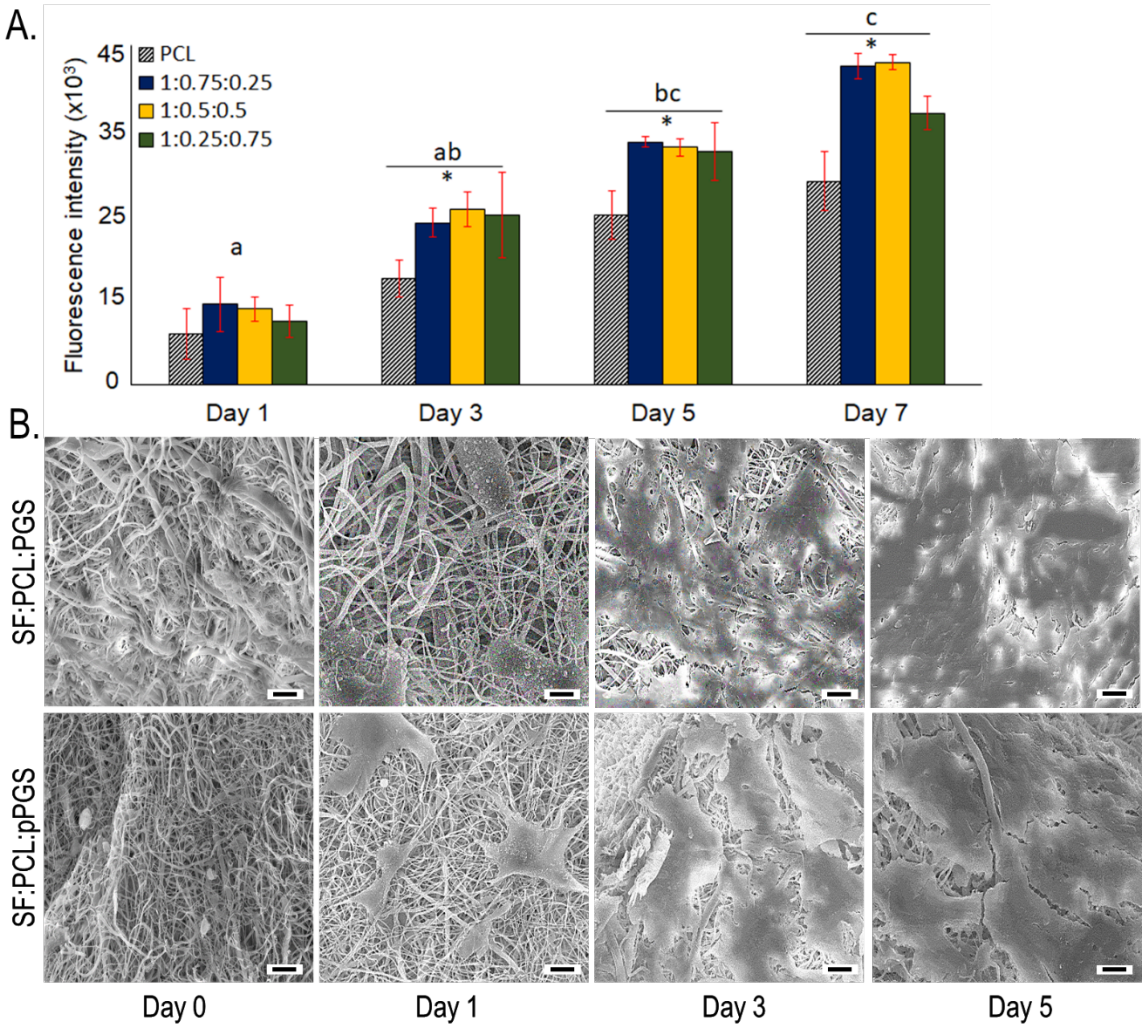

Figure 7. (A) Alamar blue cell viability assay of the SF:PCL:(p)PGS scaffolds. Values represent mean ± SD ($n=9$, $p<0.05$). a, b, c - indicate significant difference and similar values (ANOVA). * - indicates significant differences between the PCL-only and trinary electrospun mats groups (B) SEM images of HDF-TERT seeded morphology on the trinary SF:PCL:(p)PGS 1:0.5:0.5 electrospun scaffolds. Scale bar is 10 μm.

The proliferative and adhesive properties of the electrospun SF:PCL:PGS and SF:PCL:pPGS in the ratio of 1:0.5:0.5 were further assessed by fixing the fibroblast seeded scaffolds and examining their morphology by SEM imaging (Figure 7B). The SEM micrographs present fibroblasts that carry a

polygonal morphology, characteristic of healthy fibroblasts, compared to round cells, which are predominately found in fibroblasts grown on synthetic material, such as pure PCL (Figure S7). Cell attachment to the fiber surface was visibly apparent on the day of inoculation. A good surface interaction is present between the adherent cells and the electrospun fibers, as shown in the SEM images. This morphological characteristic can be attributed to the addition of the biocompatible PGS and SF protein. The cells appear to have spread quickly over the electrospun mats and are capable of expanding and covering the scaffolds within 5 days, as the SEM images display. Figure S8 displays the Cryo-SEM micrographs of FIB incisions obtained for the trinary composite fiber mats. Fibroblast ingrowth along the scaffolds fibrous network indicates complete ingrowth of the electrospun mats by day 5. These results indicate that the composite fibrous scaffolds allow for strong fibroblast attachment and good proliferation.

4. CONCLUSION

Although PCL has been extensively used for tissue engineering applications due to its good mechanical properties and its ability to mimic a number of aspects of the natural ECM architecture, its hydrophobicity makes it a least favorable candidate. To address this problem, PCL-backbone SF:PGS electrospun mats were fabricated with superior collective properties. The fibers displayed smooth morphology with controllable fiber diameter and appropriate pore size for fibroblast infiltration based on the polymerization time of PGS and tunable hydrophobicity/hydrophilicity depending on the amount of PGS and pPGS within the scaffolds. The trinary scaffolds appeared to be highly biocompatible, allowing for fibroblasts to effectively adhere and proliferate over time. The nozzle-free electrospinning technology developed, along with the straightforward SF extraction method employed, enables PCL-backbone SF:PGS fibrous scaffolds to be promising candidates as substitute constructs for skin regeneration.

ACKNOWLEDGEMENTS

The authors would like to thank Dr. Junxi Wu from the Centre for Cardiovascular Science of The University of Edinburgh for donating the cell-line used in this study. Dr. Coinneach Dover, Prof Khellil Sefiane, and Dr. Mike Davidson for sharing their expertise and allowing us access and training to the water contact angle instrument and FTIR equipment, respectively. Furthermore, we would like to recognize the Castansa Trust for their donation of the SEM (JEOL JSM-IT100) to the Radacsi research group. We would also like to thank Fergus Dingwall and Wesley Shao for their appreciated laboratory assistance. We acknowledge the use of the Cryo FIB/SEM bought with the EPSRC grant EP/P030564/1 and Thomas Glen for help with image acquisition.

REFERENCES

[1] M. Zhu, W. Li, X. Dong, X. Yuan, A.C. Midgley, H. Chang, Y. Wang, H. Wang, K. Wang, P.X. Ma, H. Wang, D. Kong, In vivo engineered extracellular matrix scaffolds with instructive niches for oriented tissue regeneration, Nat. Commun. (2019). doi:10.1038/s41467-019-12545-3.

[2] J.R. Dias, P.L. Granja, P.J. Bártolo, Advances in electrospun skin substitutes, Prog. Mater. Sci. 84 (2016) 314–334. doi:10.1016/j.pmatsci.2016.09.006.

[3] C. Cleeton, A. Keirouz, X. Chen, N. Radacsi, Electrospun Nanofibers for Drug Delivery and Biosensing, ACS Biomater. Sci. Eng. 5 (2019) 4183–4205. doi:10.1021/acsbiomaterials.9b00853.

[4] C. Wu, T. Chen, Y. Xin, Z. Zhang, Z. Ren, J. Lei, B. Chu, Y. Wang, S. Tang, Nanofibrous asymmetric membranes self-organized from chemically heterogeneous electrospun mats for skin tissue engineering, Biomed. Mater. 11 (2016) 035019. doi:10.1088/1748-6041/11/3/035019.

[5] M. Bacakova, J. Musilkova, T. Riedel, D. Stranska, E. Brynda, L. Bacakova, M. Zaloudkova, The potential applications of fibrin-coated electrospun polylactide nanofibers in skin tissue engineering, Int. J. Nanomedicine. 11 (2016) 771. doi:10.2147/IJN.S99317.

[6] K. Vig, A. Chaudhari, S. Tripathi, S. Dixit, R. Sahu, S. Pillai, V.A. Dennis, S.R. Singh, Advances in skin regeneration using tissue engineering, Int. J. Mol. Sci. 18 (2017). doi:10.3390/ijms18040789.

[7] J. Xue, T. Wu, Y. Dai, Y. Xia, Electrospinning and electrospun nanofibers: Methods, materials, and applications, Chem. Rev. 119 (2019) 5298–5415. doi:10.1021/acs.chemrev.8b00593.

[8] S. Agarwal, J.H. Wendorff, A. Greiner, Use of electrospinning technique for biomedical applications, Polymer (Guildf). 49 (2008) 5603–5621. doi:10.1016/j.polymer.2008.09.014.

[9] C.Y. Huang, K.H. Hu, Z.H. Wei, Comparison of cell behavior on pva/pva-gelatin electrospun nanofibers with random and aligned configuration, Sci. Rep. (2016). doi:10.1038/srep37960.

[10] F. Chen, D. Porter, F. Vollrath, Structure and physical properties of silkworm cocoons, J. R. Soc. Interface. 9 (2012) 2299–2308. doi:10.1098/rsif.2011.0887.

[11] C.Z. Zhou, F. Confalonieri, M. Jacquet, R. Perasso, Z.G. Li, J. Janin, Silk fibroin: Structural implications of a remarkable amino acid sequence, Proteins Struct. Funct. Genet. (2001). doi:10.1002/prot.1078.

[12] Y. Qi, H. Wang, K. Wei, Y. Yang, R.Y. Zheng, I.S. Kim, K.Q. Zhang, A review of structure construction of silk fibroin biomaterials from single structures to multi-level structures, Int. J. Mol. Sci. (2017). doi:10.3390/ijms18030237.

[13] B. Liu, Y. wei Song, L. Jin, Z. jian Wang, D. yong Pu, S. qiang Lin, C. Zhou, H. jian You, Y. Ma, J. min Li, L. Yang, K.L.P. Sung, Y. guang Zhang, Silk structure and degradation, Colloids Surfaces B Biointerfaces. 131 (2015) 122–128. doi:10.1016/j.colsurfb.2015.04.040.

[14] D. Tian, T. Li, R. Zhang, Q. Wu, T. Chen, P. Sun, A. Ramamoorthy, Conformations and Intermolecular Interactions in Cellulose/Silk Fibroin Blend Films: A Solid-State NMR Perspective, J. Phys. Chem. B. (2017). doi:10.1021/acs.jpcb.7b02838.

[15] W. Zhang, L. Chen, J. Chen, L. Wang, X. Gui, J. Ran, G. Xu, H. Zhao, M. Zeng, J. Ji, L. Qian, J. Zhou, H. Ouyang, X. Zou, Silk Fibroin Biomaterial Shows Safe and Effective Wound Healing in Animal Models and a Randomized Controlled Clinical Trial, Adv. Healthc. Mater. 6 (2017). doi:10.1002/adhm.201700121.

[16] T. Sabu, N. Neethu, M. Sneha, F. Elizabeth, Natural Polymers, Biopolymers, Biomaterials, and Their Composites, Blends, and IPNs, 2012.

[17] J.L. Ifkovits, J.J. Devlin, G. Eng, T.P. Martens, G. Vunjak-, J.A. Burdick, Biodegradable Fibrous Scaffolds

with Tunable Properties Formed from Photocrosslinkable Poly(glycerol sebacate), 1 (2010) 1878–1892. doi:10.1021/am900403k.Biodegradable.

[18] D. Mondal, M. Griffith, S.S. Venkatraman, Polycaprolactone-based biomaterials for tissue engineering and drug delivery: Current scenario and challenges, Int. J. Polym. Mater. Polym. Biomater. (2016). doi:10.1080/00914037.2015.1103241.

[19] S. Sant, A. Khademhosseini, Fabrication and Characterization of Tough Elastomeric Fibrous Scaffolds for Tissue Engineering Applications, Eng Med Biol Soc. (2010) 22–24. doi:10.1109/IEMBS.2010.5627486.Fabrication.

[20] D.N. Rockwood, R.C. Preda, T. Yücel, X. Wang, M.L. Lovett, D.L. Kaplan, Materials fabrication from Bombyx mori silk fibroin, Nat. Protoc. (2011). doi:10.1038/nprot.2011.379.

[21] D.N. Rockwood, R.C. Preda, T. Yücel, X. Wang, M.L. Lovett, D.L. Kaplan, Materials fabrication from Bombyx mori silk fibroin, Nat. Protoc. 6 (2011) 1612–1631. doi:10.1038/nprot.2011.379.

[22] Y. Wang, G.A. Ameer, B.J. Sheppard, R. Langer, A tough biodegradable elastomer., Nat. Biotechnol. 20 (2002) 602–606. doi:10.1038/nbt0602-602.

[23] N. Sasithorn, L. Martinová, Fabrication of silk nanofibres with needle and roller electrospinning methods, J. Nanomater. 2014 (2014). doi:10.1155/2014/947315.

[24] A. Keirouz, G. Fortunato, M. Zhang, A. Callanan, N. Radacsi, Nozzle-free electrospinning of Polyvinylpyrrolidone/Poly(glycerol sebacate) fibrous scaffolds for skin tissue engineering applications, Med. Eng. Phys. 71 (2019) 56–67. doi:10.1016/j.medengphy.2019.06.009.

[25] C.C. Lau, M.K. Bayazit, J.C. Knowles, J. Tang, Tailoring degree of esterification and branching of poly(glycerol sebacate) by energy efficient microwave irradiation, Polym. Chem. 8 (2017) 3937–3947. doi:10.1039/C7PY00862G.

[26] N. Amiraliyan, M. Nouri, M. Haghighat Kish, Structural characterization and mechanical properties of electrospun silk fibroin nanofiber mats, Polym. Sci. Ser. A. 52 (2010) 407–412. doi:10.1134/S0965545X10040097.

[27] Q. Zhang, S. Yan, M. Li, Silk Fibroin Based Porous Materials, Materials (Basel). 2 (2009) 2276–2295. doi:10.3390/ma2042276.

[28] J. Zhu, J. Luo, X. Zhao, J. Gao, J. Xiong, Electrospun homogeneous silk fibroin/poly (ε-caprolactone) nanofibrous scaffolds by addition of acetic acid for tissue engineering, J. Biomater. Appl. 31 (2016) 421–437. doi:10.1177/0885328216659775.

[29] C.M. Murphy, M.G. Haugh, F.J. O'Brien, The effect of mean pore size on cell attachment, proliferation and migration in collagen-glycosaminoglycan scaffolds for bone tissue engineering, Biomaterials. (2010). doi:10.1016/j.biomaterials.2009.09.063.

[30] C.M. Murphy, F.J. O'Brien, Understanding the effect of mean pore size on cell activity in collagen-glycosaminoglycan scaffolds, Cell Adhes. Migr. (2010). doi:10.4161/cam.4.3.11747.

[31] D. Gorth, T. J Webster, Matrices for tissue engineering and regenerative medicine, in: Biomater. Artif. Organs, Elsevier, 2011: pp. 270–286. doi:10.1533/9780857090843.2.270.

[32] V. Karageorgiou, D. Kaplan, Porosity of 3D biomaterial scaffolds and osteogenesis, Biomaterials. (2005). doi:10.1016/j.biomaterials.2005.02.002.

[33] K.K. Mallick, S.C. Cox, Biomaterial scaffolds for tissue engineering, Front. Biosci. - Elit. (2013). doi:10.2741/E620.

[34] E. Giebel, J. Getze, T. Röcker, A. Greiner, The importance of crosslinking and glass transition temperature for the mechanical strength of nanofibers obtained by green electrospinning, Macromol. Mater. Eng.

(2013). doi:10.1002/mame.201200080.

[35] C. Drew, X. Wang, L.A. Samuelson, J. Kumar, The Effect of Viscosity and Filler on Electrospun Fiber Morphology, in: J. Macromol. Sci. - Pure Appl. Chem., 2003. doi:10.1081/MA-120025320.

[36] H. Fong, I. Chun, D.H. Reneker, Beaded nanofibers formed during electrospinning, in: Polymer (Guildf)., 1999. doi:10.1016/S0032-3861(99)00068-3.

[37] C.J. Luo, E. Stride, M. Edirisinghe, Mapping the influence of solubility and dielectric constant on electrospinning polycaprolactone solutions, Macromolecules. (2012). doi:10.1021/ma300656u.

[38] X. Gu, X. Song, C. Shao, P. Zeng, X. Lu, X. Shen, Q. Yang, Electrospinning of poly(butylene-carbonate): Effect of solvents on the properties of the nanofibers film, Int. J. Electrochem. Sci. (2014).

[39] D. Nurwaha, W. Han, X. Wang, Investigation of a New Needleless Electrospinning Method for the Production of Nanofibers, J. Eng. Fiber. Fabr. (2018). doi:10.1177/155892501300800413.

[40] H. Niu, T. Lin, X. Wang, Needleless electrospinning. I. A comparison of cylinder and disk nozzles, J. Appl. Polym. Sci. (2009). doi:10.1002/app.30891.

[41] S. Moon, M. Gil, K.J. Lee, Syringeless Electrospinning toward Versatile Fabrication of Nanofiber Web, Sci. Rep. 7 (2017) 41424. doi:10.1038/srep41424.

[42] N. Radacsi, F.D. Campos, C.R.I. Chisholm, K.P. Giapis, Spontaneous formation of nanoparticles on electrospun nanofibres, Nat. Commun. (2018). doi:10.1038/s41467-018-07243-5.

[43] Y. Liu, K. Tian, J. Hao, T. Yang, X. Geng, W. Zhang, Biomimetic poly(glycerol sebacate)/polycaprolactone blend scaffolds for cartilage tissue engineering, J. Mater. Sci. Mater. Med. (2019). doi:10.1007/s10856-019-6257-3.

[44] S.L. Liang, X.Y. Yang, X.Y. Fang, W.D. Cook, G.A. Thouas, Q.Z. Chen, In Vitro enzymatic degradation of poly (glycerol sebacate)-based materials, Biomaterials. (2011). doi:10.1016/j.biomaterials.2011.07.080.

[45] W.P. Ye, F.S. Du, W.H. Jin, J.Y. Yang, Y. Xu, In vitro degradation of poly(caprolactone), poly(lactide) and their block copolymers: Influence of composition, temperature and morphology, React. Funct. Polym. (1997). doi:10.1016/S1381-5148(96)00081-8.

[46] K.T. Shalumon, K.H. Anulekha, K.P. Chennazhi, H. Tamura, S. V. Nair, R. Jayakumar, Fabrication of chitosan/poly(caprolactone) nanofibrous scaffold for bone and skin tissue engineering, Int. J. Biol. Macromol. (2011). doi:10.1016/j.ijbiomac.2011.01.020.

[47] A. Nadim, S.N. Khorasani, M. Kharaziha, S.M. Davoodi, Design and characterization of dexamethasone-loaded poly (glycerol sebacate)-poly caprolactone/gelatin scaffold by coaxial electro spinning for soft tissue engineering, Mater. Sci. Eng. C. 78 (2017) 47–58. doi:10.1016/j.msec.2017.04.047.

[48] Q. Lu, B. Zhang, M. Li, B. Zuo, D.L. Kaplan, Y. Huang, H. Zhu, Degradation mechanism and control of silk fibroin, Biomacromolecules. (2011). doi:10.1021/bm101422j.

[49] H.J. Jin, J. Park, V. Karageorgiou, U.J. Kim, R. Valluzzi, P. Cebe, D.L. Kaplan, Water-stable silk films with reduced β-sheet content, Adv. Funct. Mater. (2005). doi:10.1002/adfm.200400405.

[50] I. Pomerantseva, N. Krebs, A. Hart, C.M. Neville, A.Y. Huang, C.A. Sundback, Degradation behavior of poly(glycerol sebacate), J. Biomed. Mater. Res. - Part A. (2009). doi:10.1002/jbm.a.32327.

[51] W.C. Lin, N.A.M. Razali, Temporary wettability tuning of PCL/PDMS micro pattern using the plasma treatments, Materials (Basel). (2019). doi:10.3390/ma12040644.

[52] M. Ferrari, F. Cirisano, M.C. Morán, Mammalian Cell Behavior on Hydrophobic Substrates: Influence of Surface Properties, Colloids and Interfaces. (2019). doi:10.3390/colloids3020048.

[53] R.S. Kurusu, N.R. Demarquette, Surface modification to control the water wettability of electrospun mats, Int. Mater. Rev. (2019). doi:10.1080/09506608.2018.1484577.

[54] G. Wang, X. Hu, W. Lin, C. Dong, H. Wu, Electrospun PLGA-silk fibroin-collagen nanofibrous scaffolds for nerve tissue engineering, Vitr. Cell. Dev. Biol. - Anim. (2011). doi:10.1007/s11626-010-9381-4.

[55] E. Mariani, G. Lisignoli, R.M. Borzì, L. Pulsatelli, Biomaterials: Foreign bodies or tuners for the immune response?, Int. J. Mol. Sci. (2019). doi:10.3390/ijms20030636.

[56] C. Frantz, K.M. Stewart, V.M. Weaver, The extracellular matrix at a glance, J. Cell Sci. (2010). doi:10.1242/jcs.023820.

[57] P. Azari, P. Azari, S. Hosseini, B.P. Murphy, S.O. Martinez-Chapa, Electrospun Biopolyesters: Hydrophobic Scaffolds with Favorable Biological Response, J. Public Heal. Int. 1 (2018) 5–9. doi:10.14302/issn.2641-4538.jphi-18-1975.

[58] B. Dhandayuthapani, Y. Yoshida, T. Maekawa, D.S. Kumar, Polymeric scaffolds in tissue engineering application: A review, Int. J. Polym. Sci. (2011). doi:10.1155/2011/290602.

[59] T. Roy, P. Maity, A. Rameshbabu, B. Das, A. John, A. Dutta, S. Ghorai, S. Chattopadhyay, S. Dhara, Core-Shell Nanofibrous Scaffold Based on Polycaprolactone-Silk Fibroin Emulsion Electrospinning for Tissue Engineering Applications, Bioengineering. 5 (2018) 68. doi:10.3390/bioengineering5030068.

[60] W. Zhou, Y. Feng, J. Yang, J. Fan, J. Lv, L. Zhang, J. Guo, X. Ren, W. Zhang, Electrospun scaffolds of silk fibroin and poly(lactide-co-glycolide) for endothelial cell growth, J. Mater. Sci. Mater. Med. (2015). doi:10.1007/s10856-015-5386-6.

[61] I. Ghaeli, M.A. De Moraes, M.M. Beppu, K. Lewandowska, A. Sionkowska, F. Ferreira-Da-Silva, M.P. Ferraz, F.J. Monteiro, Phase behaviour and miscibility studies of collagen/silk fibroin macromolecular system in dilute solutions and solid state, Molecules. (2017). doi:10.3390/molecules22081368.

[62] V. De Sanctis, A. Soliman, S. Bernasconi, L. Bianchin, G. Bona, M. Bozzola, F. Buzi, C. De Sanctis, G. Tonini, F. Rigon, E. Perissinotto, Primary dysmenorrhea in adolescents: Prevalence, impact and recent knowledge, Pediatr. Endocrinol. Rev. 13 (2015) 512–520. doi:10.1002/term.

[63] B. Xu, Y. Li, C. Zhu, W.D. Cook, J. Forsythe, Q. Chen, Fabrication, mechanical properties and cytocompatibility of elastomeric nanofibrous mats of poly(glycerol sebacate), Eur. Polym. J. 64 (2015) 79–92. doi:10.1016/j.eurpolymj.2014.12.008.

[64] S. Kandhasamy, S. Perumal, B. Madhan, N. Umamaheswari, J.A. Banday, P.T. Perumal, V.P. Santhanakrishnan, Synthesis and Fabrication of Collagen-Coated Ostholamide Electrospun Nanofiber Scaffold for Wound Healing, ACS Appl. Mater. Interfaces. 9 (2017) 8556–8568. doi:10.1021/acsami.6b16488.